



1
2
3
4
5
6
7
8
9
10
11
12
13
14
15
16
17
18
19
20
21
22
23
24
25
26
27
28
29
30
31
32
33
34
35
36
37
38
39
40
41
42
43
44
45
46
47
48
49
50

Self-sustained Oscillations in the Atmosphere (0 – 110 km) at Long Periods

Dirk Offermann(1), Christoph Kalicinsky(1), Ralf Koppmann(1), and Johannes
Wintel(1,2)

- (1) Institut für Atmosphären-und Umweltforschung, Bergische Universität Wuppertal,
Wuppertal, Germany
(2) Now at Elementar Analysensysteme GmbH, Langenselbold, Germany

Corresponding author: Dirk Offermann, (offer@uni-wuppertal.de)

- Key Points: - multi-decadal oscillations in GCM and measurements (up to 341 yr)
- self-sustained oscillations linked to the atmosphere basic dynamics
- vertical amplitude and phase structure similar for all oscillation periods

Abstract



51 Self-generated (self-sustained) oscillations have been observed in measured atmospheric
52 data at multi-annual periods. These oscillations are also present in General Circulation
53 Models even if their boundary conditions with respect to solar cycle, sea surface temperature,
54 and trace gas variability are kept constant. The present analysis contains temperature
55 oscillations with periods from below 5 yr up to 341 yr in an altitude range from the Earth's
56 surface to the lower thermosphere (110 km). The periods are quite robust as they are found to
57 be the same in different model calculations and in atmospheric measurements. The
58 oscillations show vertical profiles with special structures of amplitudes and phases. They form
59 layers of high / low amplitudes that are a few dozen km wide. Within the layers the data are
60 correlated. Adjacent layers are anticorrelated. A vertical displacement mechanism is indicated
61 with displacement heights of a few 100 metres. Vertical profiles of amplitudes and phases of
62 the various oscillation periods as well as their displacement heights are surprisingly similar.
63 The oscillations are related to the thermal and dynamical structure of the middle atmosphere.
64 These results are from latitudes/longitudes in Central Europe.

65
66
67
68

69 Short summary

70

71 Atmospheric oscillations with periods up to several 100 years exist at altitudes up to 110
72 km. They are also seen in computer models (GCM) of the atmospheric. They are often
73 attributed to external influences from the sun, from the oceans, or from atmospheric
74 constituents. This is difficult to verify as the atmosphere cannot be manipulated in an
75 experiment. However, a GCM can be changed arbitrarily! Doing so we find that long period
76 oscillations can be excited internally in the atmosphere.

77
78
79

80

81

82

83

84

85

86

87

88

89

90

91

92

93

94

95

96

97

98 1 Introduction

99

100 Multi-annual oscillations with periods between 2 and 11 years have frequently been discussed
101 for the atmosphere and the ocean. Major examples are the Quasi-Biennial Oscillation (QBO),



102 solar cycle related variations near 11 years and 5.5 years, and the El Nino/Southern
103 Oscillation (ENSO). (For references see for instance Offermann et al., 2015.)

104 Self-excited oscillations in the ocean of such periods have been described for instance by
105 White and Liu (2008). Self-excited oscillations in the atmosphere with periods between 2.2
106 and 5.5 yr have been shown in a large altitude regime by Offermann et al. (2015). Their
107 periods are surprisingly robust, i.e. there is little change with altitude. They are also present in
108 general circulation models, the boundaries of which are kept constant.

109 Oscillations of much longer periods in the atmosphere and the ocean have also been
110 reported. Biondi et al. (2001) found bi-decadal oscillations in local tree ring records that date
111 back several centuries. Kalicinsky et al. (2016, 2018) recently presented a temperature
112 oscillation near the mesopause with a period near 25 years which may be interpreted as a self-
113 excited oscillation. Low-frequency oscillations (LFO) on local and global scales in the multi-
114 decadal range (50-80 yr) have been discussed several times (e.g., Schlesinger and Ramankutty
115 (1994); Minobe (1997); Polyakov et al.(2003); Dai et al.(2015); Dijkstra et al.(2005)). Some
116 of these results were intensively discussed as internal variability of the atmosphere-ocean
117 system, for instance as the internal interdecadal modes AMV (Atlantic Multidecadal
118 Variability) and PDO/IPO (Pacific Decadal Oscillation/Interdecadal Pacific Oscillation) (e.g.
119 Meehl et al., 2013; 2016; Lu et al., 2014; Deser et al., 2014; Dai et al., 2015.) Multidecadal
120 variations (40-80 years) of Arctic-wide surface air temperatures were, however, related to
121 solar variability by Soon (2005). Some of these long period variations have been traced
122 backwards for two or more centuries (Minobe, 1997; Biondi et al., 2001; Mantua and Hare,
123 2002; Gray et al., 2004). Multidecadal oscillations have also been discussed extensively as
124 internal climatic variability in the context of the long term climate change (temperature
125 increase) in the IPCC AR5 Report (e.g. Flato et al., 2013).

126 Even longer periods of oscillations in the ocean and the atmosphere have also been
127 reported. Karnauskas et al. (2012) find centennial variations in three general circulation
128 models of the ocean. These variations occur in the absence of external forcing, i.e. they show
129 internal variabilities on the centennial time scale. Internal variability in the ocean on a
130 centennial scale is also discussed by Latif et al. (2013) on the basis of model simulations.
131 Measured data of a 500 year quasi-periodic temperature variation are shown by Xu et al.
132 (2014). They analyze a more than 5000 year long pollen record in East Asia. Very long
133 periods are found by Paul and Schulz (2002) in a climate model. They obtain internal
134 oscillations with periods of 1600-2000 years.

135 All long period oscillations cited here refer to temperatures of the ocean or the land/ocean
136 system. It is emphasized that on the contrary the self-excited multi-annual oscillations
137 described by Offermann et al. (2015) and those discussed in the present paper are properties
138 of the atmosphere, and exist in a large altitude regime between the ground and 110 km
139 altitude. They are not linked to the ocean.

140 In the present paper the work of Offermann et al. (2015) is extended to multi-decadal and
141 centennial periods. Internal oscillations in the atmosphere are studied in three general
142 circulation models. The analysis is locally constrained (Central Europe), but vertically
143 extended up to 110 km. The model boundary conditions (sun, ocean, trace gases) are kept
144 constant. The results of model runs with HAMMONIA, WACCM, and ECHAM6 were made
145 available to us. They simulate 34 years, 150 years, and 400 years of atmospheric behavior,
146 respectively. The corresponding results are compared to each other. Most of the analyses are
147 performed for atmospheric temperatures.

148 In Section 2 of this paper the three models are described and the analysis method is
149 presented. In Section 3 the oscillations obtained from the three models are compared. The
150 vertical structures of the periods, amplitudes, and phases of the self-sustained oscillations are
151 described. In Section 4 the results are discussed. Section 5 gives a summary and some
152 conclusions.



153
154
155
156
157
158
159
160
161
162
163
164
165
166
167
168
169
170
171
172
173
174
175
176
177
178
179
180
181
182
183
184
185
186
187
188
189
190
191
192
193
194
195
196
197

2 Model data and their analysis

2.1 Self-sustained oscillations and their vertical structures

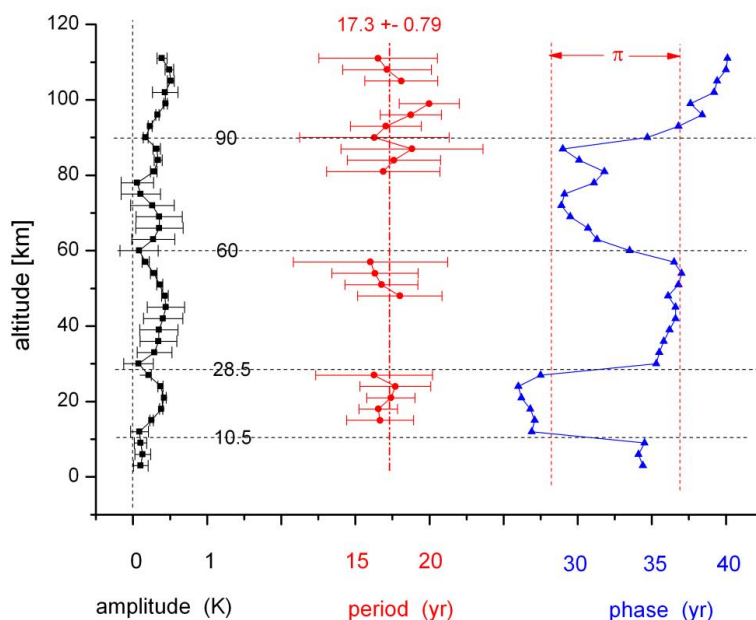
In an earlier paper (Offermann et al., 2015) multi-annual oscillations with periods of about 2 - 5 years have been described at altitudes up to 110 km. These were found in temperature data of HAMMONIA model runs (see below). They were present in the model even if the model boundary conditions (solar irradiance, sea-surface temperatures and sea ice, boundary values of green-house gases) were kept constant. Therefore they were interpreted as self-sustained (self-excited) oscillations. The periods were found to be quite robust as they did not change much with altitude. Robust periods are typical of self-excited oscillations (Pikovsky et al., 2003). The oscillations showed particular vertical structures of amplitudes and phases. Amplitudes did not increase exponentially with altitude as they do with atmospheric waves. They rather varied with altitude between maximum and near zero values in a nearly regular manner. Phases showed jumps of about 180° at the altitudes of the amplitude minima, and were about constant in between. There were indications of synchronization of amplitudes and phases.

The periods analyzed in the earlier paper have been restricted to below 5.5 yr. Much longer periods have been described in the literature. It is therefore of interest to see whether such longer periods could also be self-excited in the models.

Figure 1 shows an example of such temperature structures for an oscillation with a period of 17.3 ± 0.8 years obtained from the HAMMONIA model discussed below. This picture is typical of the oscillations in Offermann et al. (2015) and of the oscillations discussed in the present paper. The periods at the various altitudes are close to their mean value even though the error bars are fairly large. There is no indication of systematic altitude variations, and therefore the mean is taken as a first approximation. At some altitudes the periods could not be determined. In these cases the periods were prescribed by the mean of the derived periods (dash-dotted red vertical line, 17.3 yr) to obtain approximate amplitudes and phases at these altitudes (see Offermann et al., 2015). Details of the derivation of periods, amplitudes, and phases are given in Section 3.

2.2 HAMMONIA

The HAMMONIA model (Schmidt et al., 2006) is based on the ECHAM5 general circulation model (Röckner et al., 2006), but extends the domain vertically to 2×10^{-7} hPa, and is coupled to the MOZART3 chemistry scheme (Kinnison et al., 2007). The simulation analyzed here was run at a spectral resolution of T31 with 119 vertical layers. The relatively high



198
199

200 Fig.1 Vertical structures of self-sustained oscillation periods near 17.3 ± 0.8 yr from
201 HAMMONIA temperatures.

202 Missing period values could not be derived from the data. They were prescribed as the mean
203 value 17.3 yr (dash-dotted vertical red line, see text and Section 3.2). Phases are relative
204 values.

205

206 vertical resolution of less than 1 km in the stratosphere allows an internal generation of the
207 QBO. Here we analyze the simulation (with fixed boundary conditions) that was called “Hhi-
208 max” in Offermann et al. (2015), but instead of only 11 we use 34 simulated years. Further
209 details of the simulation are given by Schmidt et al. (2010).

210 An example of the HAMMONIA data is given in Fig.2 for 0 km and 3 km altitudes. The
211 HAMMONIA data were searched for self-sustained oscillations up to 110 km. The detailed
212 analysis is described below (Section 3.2). Nine oscillations were identified with periods
213 between 5.3 yr and 28.5 yr. They are listed in Table 2. The oscillation shown in Fig. 1 (17.3
214 yr) is from about the middle of this range.

215

216

217 2.3 WACCM

218

219 Long runs with chemistry-climate models (CCMs) having restricted boundary conditions
220 are not frequently available. A model run much longer than 34 years became available from
221 the CESM-WACCM4 model. This 150 year run was analyzed from the ground up to 108 km.
222 The model experiments are described in Hansen et al. (2014). Here, the experiment with
223 monthly varying constant climatological SSTs and sea ice has been used. Other boundary
224 conditions such as Greenhouse Gases (GHG) and Ozone Depleting Substances (ODP) were
225 kept constant at 1960 values.



226 Solar cycle variability, however, was not kept constant during this model experiment.
227 Spectrally resolved solar irradiance variability as well as variations of the total solar
228 irradiance and the F10.7cm solar radio flux were used from 1955 to 2004 from Lean et al.
229 (2005). Thereafter solar variations from 1962-2004 were repeated several times to reach 150
230 years in total. Details are given in Matthes et al. (2013).

231 The WACCM data were analyzed for self-excited oscillations in the same manner as the
232 HAMMONIA data. Here, the emphasis is on longer periods. Besides many shorter
233 oscillations, nine oscillations with periods of more than 20 years were found. The longest
234 period is 147 years. These results are included to Table 2.

235 .

236

237 2.4 ECHAM6

238

239 The longest computer run available to us, covering 400 years, is from ECHAM6. ECHAM6
240 (Stevens et al., 2013) is the successor of ECHAM5, the base model of HAMMONIA. Major
241 changes relative to ECHAM5 include an improved representation of radiative transfer in the
242 solar part of the spectrum, a new description of atmospheric aerosol, and a new representation
243 of the surface albedo. While the standard configuration of ECHAM5 used a model top at 10
244 hPa, this was extended to 0.01 hPa in ECHAM6. As the atmospheric component of the Max-
245 Planck-Institute Earth System Model (MPI-ESM, Giorgetta et al., 2013) it has been used in a
246 large number of model intercomparison studies related to the Coupled Model Intercomparison
247 Project phase 5 (CMIP5). The ECHAM6 simulation analyzed here was run at T63 spectral
248 resolution with 47 vertical layers (not allowing for an internal generation of the QBO). All
249 boundary conditions were fixed to constant values, taken as an average of the years 1979 to
250 2008.

251 The temperature data were analyzed as the other data sets described above. Eighteen
252 oscillation periods longer than 20 yr were obtained (Table 2), with the typical vertical
253 structures of self-sustained oscillations. The longest period is 341.2 ± 37.2 yr

254 A summary of the model properties is given in Table 1. All analyses in this paper are for
255 Central Europe. The vertical model profiles are for 50°N , 7°E .

256

257

258

259 3 Model results

260

261

262 3.1 Vertical correlations of atmospheric temperatures

263

264 Figure 1 indicates that there are some vertical correlation structures in the atmospheric
265 temperatures. This was studied in detail for the HAMMONIA and ECHAM6 data.

266 Ground temperature residues from the HAMMONIA run 38123 (34 years) are shown in
267 Fig. 2 (black squares). The mean temperature is 281.89 K, which was subtracted from the
268 model data. The boundary conditions (sun, ocean, green house gases) have been kept constant
269 , as discussed above. The temperature fluctuations thus show the internal atmospheric
270 variability (standard deviation is $\sigma = \pm 0.62$ K). This variability is frequently termed
271 “(climate) noise” in the literature. It will be checked whether this notion is justified in the
272 present case.

273 Also shown in Fig. 2 are the corresponding HAMMONIA data for 3 km altitude. The mean
274 temperature is 266.04 K, the standard deviation is $\sigma = \pm 0.41$ K. The statistical error of these
275 two standard deviations is about 12%. Hence the internal variances at the two altitudes are

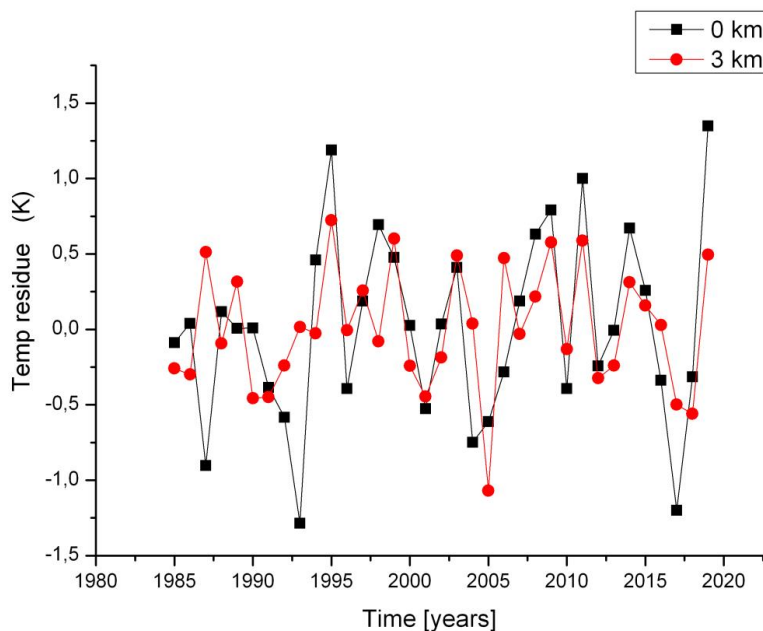


276 statistically different. This suggests that there may be a vertical structure in the variability that
277 should be analyzed.

278 The data sets in Fig. 2 show large changes within short times (2-4 years). Sometimes these
279 changes are similar at the two altitudes. The variability of HAMMONIA thus appears to
280 contain an appreciable high frequency component and thus needs to be analyzed as well for
281 vertical as for spectral structures.

282 Temperatures at layers 3 km apart in altitude were therefore correlated with those at 42 km
283 as a reference altitude (near stratopause). The results are shown in Fig.3 for HAMMONIA
284 model run up to 105 km (red dots). A corresponding analysis for the much longer model run
285 of ECHAM6 is also shown (black squares, up to 78 km). Two important results are obtained:
286 1) There is an oscillatory vertical structure in the correlation coefficient r with two maxima in
287 the upper stratosphere and upper mesosphere/lower thermosphere, respectively, and two
288 minima in the lower stratosphere and in the mesosphere, respectively (for HAMMONIA).
289 The correlations are highly significant near the upper three of these extrema (see the 95%
290 lines in Fig. 3 for HAMMONIA; the significance is much better for ECHAM6). 2.) The
291 correlations in the two different data sets are nearly the same above the troposphere. This is
292 remarkable because the two sets cover time intervals very different in length (34 years vs 400
293 years, respectively). Therefore, the correlation structure appears to be a basic property of the
294 atmosphere (see below).

295
296
297
298
299



300
301
302
303
304

Fig.2 HAMMONIA temperature residues at 0 km and 3 km altitude with fixed boundary conditions (see text). Mean temperatures of 281.89 K (0 km) and 266.04 K (3 km) have been subtracted from the model temperatures.

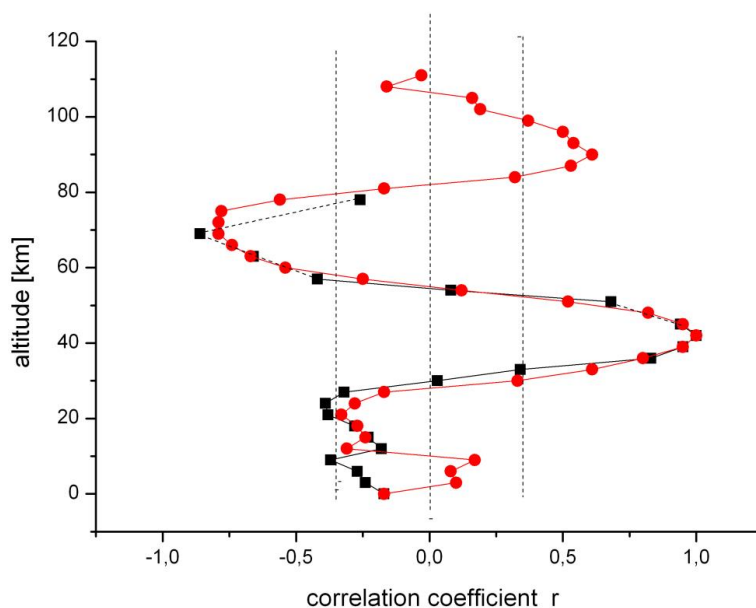


305
306
307
308
309
310
311
312
313
314
315
316
317
318
319
320
321
322

The correlations suggest that the fluctuations in the atmosphere (or part of them) are somehow “synchronized” at adjacent altitude levels. A vertical (layered) structure might therefore be present in the magnitude of the fluctuations, too. This was studied by means of the standard deviations σ of the temperatures T , the result is shown in Fig. 4. There is indeed a vertical structure with fairly pronounced layers.

The HAMMONIA data used for Fig.4 were annual data that have been smoothed by a four point running mean. This was done to reduce the influence of high frequency “noise” mentioned above, which is substantial (a factor of 2).

The layered structures shown in Fig. 3 and 4 are not unrelated. This can be seen in Fig. 4 that also gives the vertical correlations r (Fig.3) for comparison. The horizontal dashed lines indicate that the maxima of the standard deviations occur near the extrema of the correlation profile in the stratosphere and lower mesosphere. This means that the fluctuations in adjacent σ maxima (and in adjacent layers) are anticorrelated. Surprisingly these anticorrelations are also approximately seen in the amplitude and phase profiles of Fig.1 that are typical of all oscillations (see below).



323
324
325
326
327
328
329
330
331
332

Fig.3 Vertical correlation of temperatures in HAMMONIA (red dots) and ECHAM6 (black squares). Reference altitude is 42 km ($r = 1$). Vertical dotted lines show 95% significance for Hammonia.

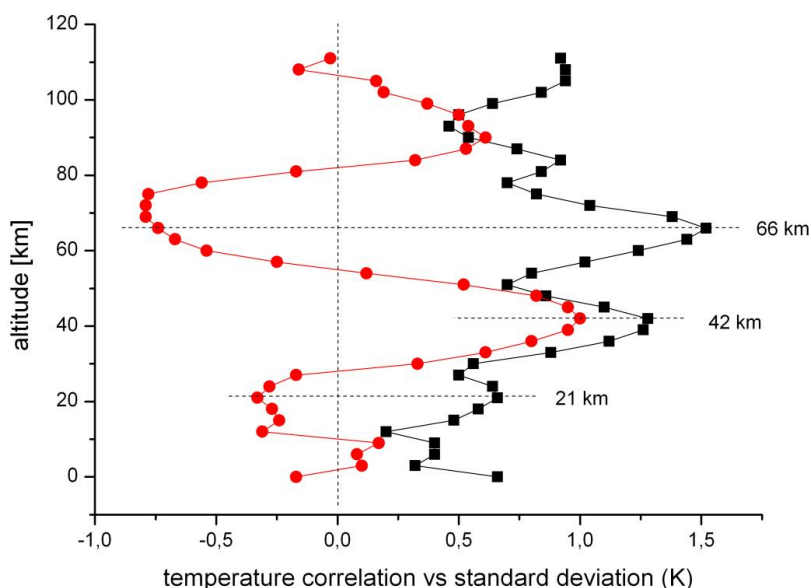
The ECHAM6 data have been analyzed in the same way as the HAMMONIA data, including a smoothing by a 4 point running mean. The data cover the altitude range of 0 -78 km for a 400 year simulation. The results are very similar to those of



333 HAMMONIA. This is shown in Fig.5 that gives vertical profiles of standard deviations and of
334 vertical correlations of the smoothed ECHAM6 data, and is to be compared to the
335 HAMMONIA results in Fig. 4. The two upper maxima of standard deviations are again
336 anticorrelated.

337 It is apparently a basic property of the atmosphere's internal variability to be organized in
338 some kind of "layers", and that adjacent layers are anti-correlated. It appears therefore
339 questionable whether the internal variability may be termed "noise", as is frequently done in
340 the literature.

341
342



343
344

345 Fig.4 HAMMONIA temperatures: Comparison of standard deviations (black squares,
346 multiplied by 2) and correlation coefficients (red dots, see Fig. 3). For details see text.

347
348

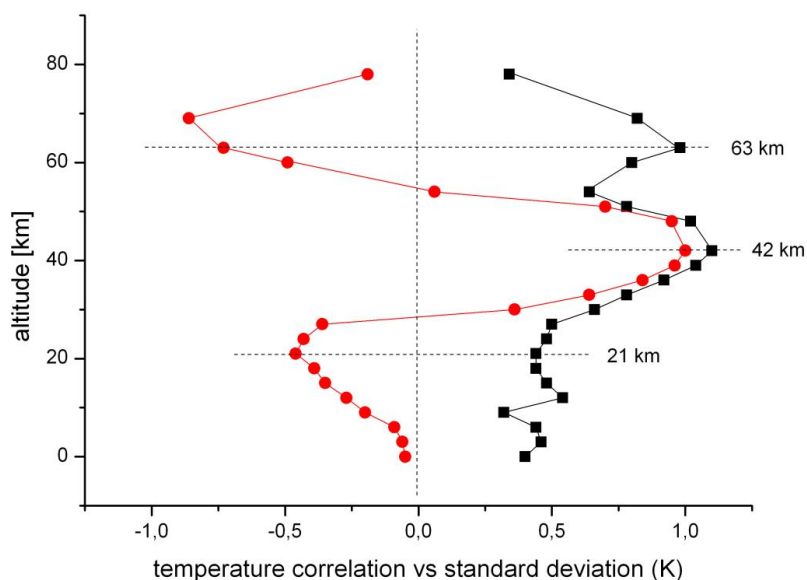
349 3.2 Time structures

350

351 The correlations/anticorrelations concern temporal variations of temperatures. This suggests
352 a search for some kind of regular (ordered) structure in the time series, as well. Therefore in a
353 first step, FFT analyses have been performed for all HAMMONIA altitude levels (3 km
354 apart). The results are shown in Fig.6 that gives amplitudes for the period range of 4 - 34
355 years versus altitude. Also in this picture, the amplitudes show a layered structure. In addition
356 an ordered structure in the period domain is also indicated. There are increased or high
357 amplitudes near certain period values, for instance at the left and right hand side and in the
358 middle of the picture. A similar result is obtained for the ECHAM6 data shown in Fig.7 for
359 the longer periods of 10-400 years. The layered structure in altitude is clearly seen, and so are
360 the increased amplitudes near certain period values. Obviously, the computer simulations
361 contain periodic temperature oscillations, the amplitudes of which show a vertically layered



362 order. Because the boundary conditions of the computer runs were kept constant, these
363 oscillations cannot be excited from the outside. They are therefore interpreted as self-excited
364 (self-sustained) oscillations, and thus as intrinsic properties of the atmosphere
365
366
367



368 Fig.5 ECHAM6 temperatures: Comparison of standard deviations (black squares,
369 multiplied by 2) and correlation coefficients (red dots). For details see text.
370
371
372

373 The amplitudes shown in Fig.6 and 7 are relative values, and the resolution of the spectra is
374 quite limited. Therefore a more detailed analysis is required. For this purpose the Lomb-
375 Scargle Periodogram (Lomb 1976; Scargle 1982) is used. As an example Fig 8 shows the
376 mean Lomb-Scargle Periodogram in the period range 20 – 100 years for the ECHAM6 data.
377 For this picture Lomb-Scargle spectra were calculated for all ECHAM6 layers separately, and
378 the mean spectrum of all altitudes was determined. The power of the periodogram gives the
379 reduction in sum of squares when fitting a sinusoid to the data (Scargle 1982), i.e. it is
380 equivalent to a harmonic analysis using least square fitting of sinusoids. The power values are
381 normalized by the variance of the data to obtain comparability of the layers with different
382 variance. Quite a number of spectral peaks are seen between 20 and 60 years period. Further
383 oscillations appear to be present around 100 years and at even longer periods (not shown here
384 as they are not sufficiently resolved).

385 We compared the mean result for the ECHAM6 data with 10000 representations of noise.
386 One representation covers 47 atmospheric layers. For each representation we took noise from
387 a Gaussian distribution for each atmospheric layer independently, and calculated a mean
388 Lomb-Scargle Periodogram for every representation in the same way as for the ECHAM6
389 data. The red line in Fig. 8 shows the average of all of these mean periodograms. As expected
390 for the average of all representations the peaks cancel, and one gets an approximately constant



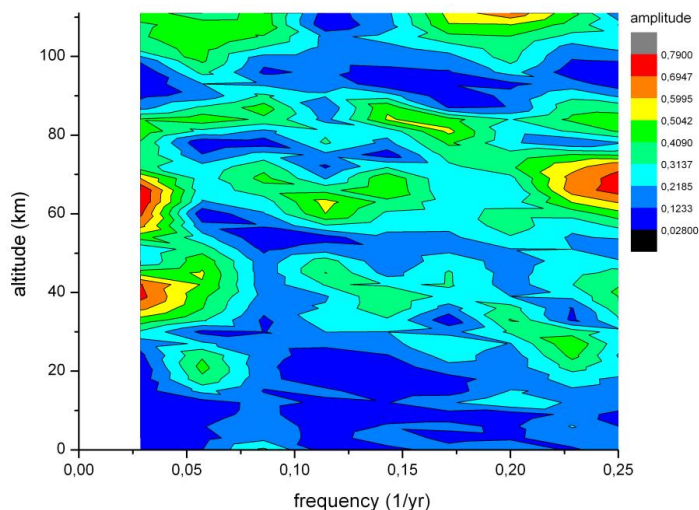
391 value for all periods. A single representation typically shows one or several peaks above this
392 mean level. The red dashed line gives the upper 2σ level, i.e. the mean plus 2σ . As the mean
393 Lomb-Scargle Periodogram for the ECHAM6 data shows several peaks clearly above this
394 upper 2σ level, this mean periodogram is significantly different from that of independent
395 noise. Therefore, the conclusion is that independent noise at the different atmospheric layers
396 alone cannot explain the observed periodogram showing large remaining peaks after
397 averaging. A coupling mechanism between the layers has to be present to explain the
398 observed mean Lomb-Scargle Periodogram for the ECHAM6 data.

399 It might be considered appropriate to use red noise instead of white noise in this analysis.
400 We therefore calculated the sample autocorrelation at a lag of 1 year for the different
401 ECHAM6 altitudes. These values were found to be very close to zero and, thus, we used
402 Gaussian noise in our analysis.

403 The period values shown in Fig. 8 agree with those given for ECHAM6 in Table 2 which
404 are from the harmonic analysis described next. The agreement is within the error bars given in
405 Table 2 (except for 24.3).

406 A spectral analysis as that in Fig.8 was also performed for the HAMMONIA temperatures.
407 It showed the periods of 5.3 yr and 17.3 yr above the 2σ level. These values agree within
408 single error bars with those given in Table 2. All peaks found to be significant (in different
409 analyses) are marked by heavy print in Table 2.

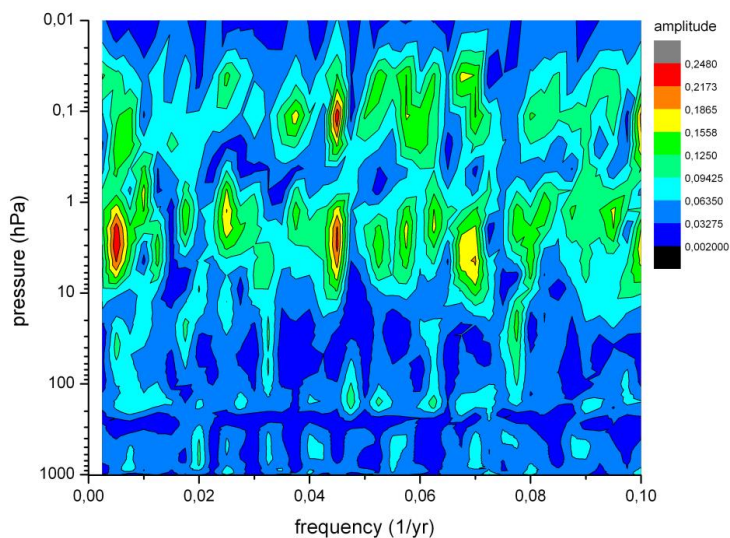
410
411



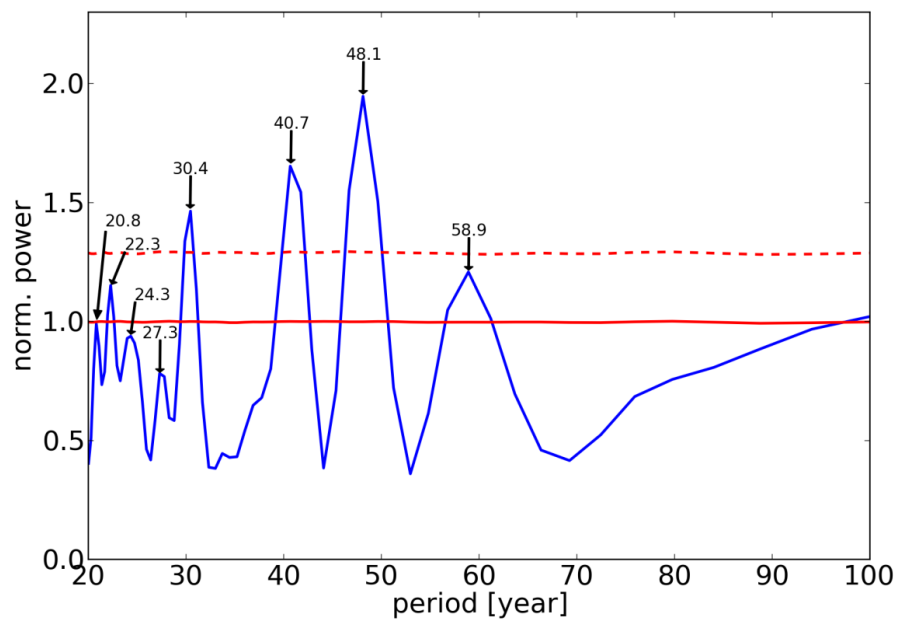
412
413 Fig. 6 Self-excited temperature oscillations in the HAMMONIA model.
414 FFT amplitudes are shown in dependence on altitude and frequency (periods 4 – 34 yr).
415 Colour code of amplitudes is in arbitrary units.

416
417

418 The Lomb-Scargle spectra (in their original form) do not reveal the phases of the oscillations.
419 We have therefore added harmonic analyses to our data series. This was done by stepping
420 through the period domain in steps 10% apart. In each step we looked for the largest near-by
421 sinus oscillation peak. This was done by means of an ORIGIN search algorithm (ORIGIN Pro
422 8G, Levenberg-Marquardt algorithm) that yielded optimum values for period, amplitude, and
423 phase. The results are a first approximation, though, because only one period was fitted at a
424 time, instead of the whole spectrum. Also, the 10% grid may be sometimes too coarse.



425
426 Fig. 7 Self-excited temperature oscillations in the ECHAM6 model.
427 FFT amplitudes are shown in dependence on altitude and frequency (periods 10 – 400 yr).
428 Colour code of amplitudes is in arbitrary units.
429



430
431
432 Fig.8 Self-excited temperature oscillations in the ECHAM6 model
433 Lomb-Scargle periodogram is given for periods of 20 – 100 years. Dashed line indicates
434 significance at the 2σ level (see text).

435



436

437

438

439

440

441

442

443

444

445

446

447

448

449

450

This analysis was performed for all altitude levels available. Figure 1 shows an example for the HAMMONIA temperatures from 3-111 km for periods around 15 – 20 years. The middle track (red dots) shows the periods with their error bars, the left side shows the amplitudes, and the right side the phases. The mean of all periods is 17.3 ± 0.79 years. There are several altitudes where the harmonic analysis does not give a period. This may occur if an amplitude is very small or if there is a near-by period with a strong amplitude that masks the smaller one. At these altitudes the periods were interpolated for the fit (dash-dotted vertical line). The mean of the derived periods (17.3 yr) is used as an estimated interpolation value. This is because the derived periods do not deviate too much from the mean value. This procedure allows to obtain estimated amplitude and phase values for instance in the vicinity of the amplitude minima. That is important because at these altitudes large phase changes are frequently observed. The harmonic analysis algorithm calculates an amplitude and phase if a prescribed (estimated) period is provided.

451

452

453

454

455

456

457

458

459

The right track in Fig. 1 shows the phases of the oscillations. The special feature about this vertical profile is its steplike structure with almost constant values in some altitudes and a subsequent fast change somewhat higher to some other constant level. These changes are by about 180° (π), i.e. the temperatures above and below these levels are anti-correlated. At these levels the temperature amplitudes (left track) are minimum, with maxima in between. These maxima occur near the altitudes of the maxima of the temperature standard deviations in Fig. 4 that are anti-correlated in adjacent layers. The phase steps in Fig. 1 approximately fit to this picture. They suggest that the layer anti-correlation discussed above is at least in part due to the phase structure of the self-sustained oscillations in the atmosphere.

460

461

462

463

464

This important result was checked by an analysis of other oscillations contained in the HAMMONIA data series. Nine self-sustained oscillations with periods between 5.34 years and 28.5 years were obtained by the analysis procedure described above. They are listed in Table 2, and all show vertical profiles similarly as in Fig. 1.

465

466

467

468

469

470

471

472

Figure 1 shows that at different altitudes the periods are somewhat different. They cluster, however, quite closely about their mean value of 17.3 yr. This clustering about a mean value is found for all periods listed in Table 2. This is shown in detail in Fig. 9 and 10 which give the number of periods found at different altitudes in a fixed period interval. The clusters are separated by major gaps, as is indicated by vertical dashed lines (black). This suggests to use a mean period value as an estimate of the oscillation period representative for all altitudes. The mean period values are given above each cluster in red, together with a red solid vertical line. A few clusters are not very pronounced, and hence the corresponding mean period values are unreliable (e.g. 22.8 yr, see the increased standard deviations in Table 2).

473

474

475

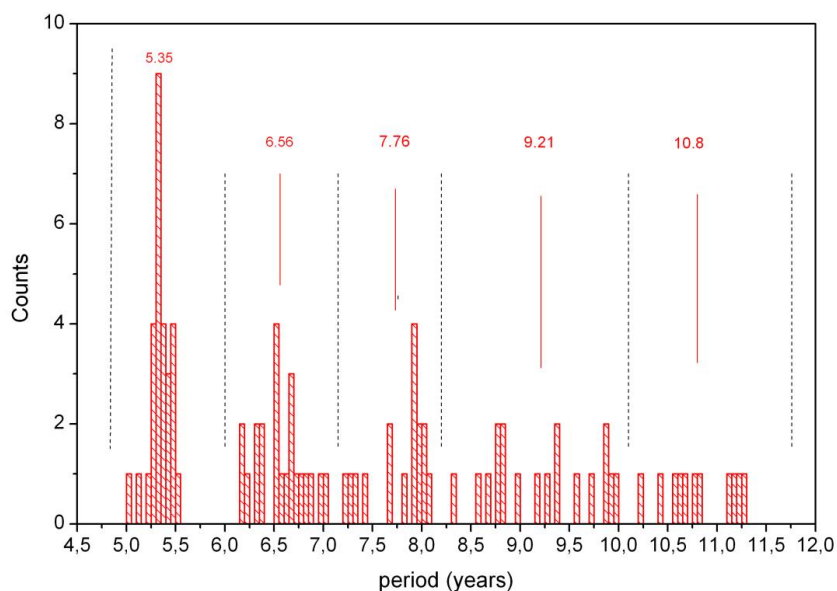
476

477

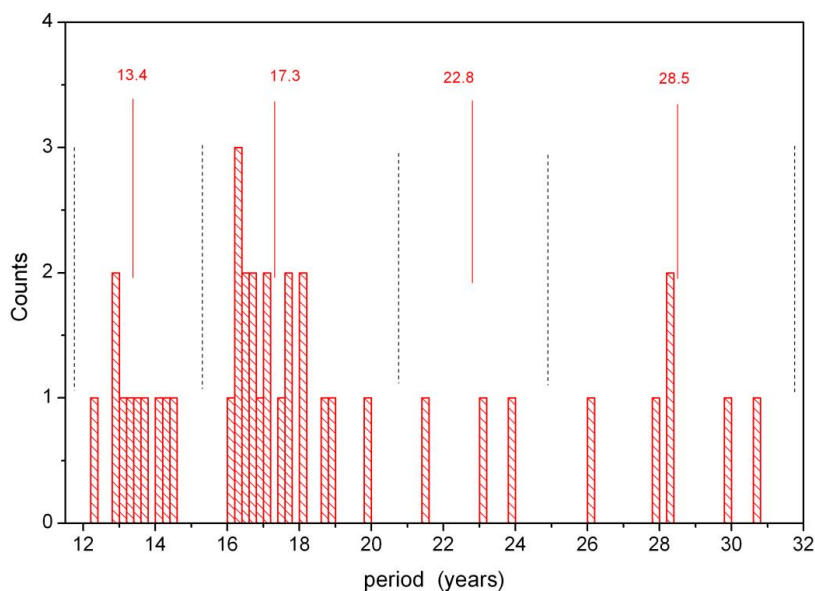
ECHAM6 - data are used in the present paper to analyze much longer time windows (400 years) than that of HAMMONIA (34 years). Results shown in Fig. 3, 5, and 7 are quite similar to those of HAMMONIA. Harmonic analysis of self-sustained oscillation periods was performed in the same way as for HAMMONIA. Eighteen periods were found longer than 20 years and have been included to Table 2. Shorter periods are not shown here as that range



478 is covered by HAMMONIA. The amplitude and phase structures of these are very similar to



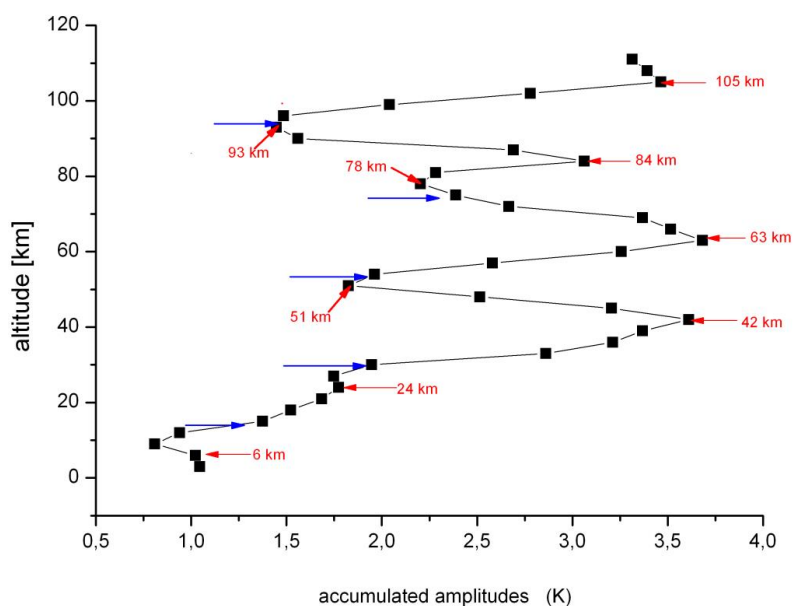
479
480 Fig.9 Number of oscillations counted in a fixed period interval at periods 4.75 – 11.75 years.
481 Interval is 0.05 years. (HAMMONIA)



482
483 Fig.10 Number of oscillations counted in a fixed period interval at periods 11.75 – 31.75
484 years. Interval is 0.2 years. (HAMMONIA)



485
486 those of HAMMONIA. The cluster formation about the mean period values is also obtained
487 for ECHAM6 and looks quite similar to Fig.9 and 10.
488 The vertical amplitude and phase profiles of the mean periods given in Table 2 all show
489 intermittent amplitude maxima/minima, and step-like phase structures. They in general look
490 very similar to Fig.1. We have calculated the accumulated amplitudes (sums) from all of these
491 profiles at all altitudes. They are shown in Fig.11 (for HAMMONIA). They clearly show a
492 layered structure similar to the temperature standard deviations in Fig 4, with maxima at
493 altitudes close to those of the standard deviation maxima. The figure also closely corresponds
494 to the amplitude distribution shown in Fig.1, with maxima and minima occurring at similar
495 altitudes in either picture.
496



497
498
499 Fig. 11 Self-excited temperature oscillations in the HAMMONIA model.
500 Accumulated amplitudes are shown vs altitude for periods of 5.3 – 28.5 years (see Table 2).
501 Blue horizontal arrows show mean altitudes of phase jumps. Red arrows indicate altitudes of
502 maxima and minima.

503
504
505 Accumulated amplitudes have also been calculated for the ECHAM6 periods, and very
506 similar results are obtained as for HAMMONIA. The similarity is already indicated in Fig.3
507 above 15 km. The correlation of the HAMMONIA and ECHAM6 curves above this altitude
508 has a correlation coefficient of 0.97. This is remarkable because many more oscillations are
509 contained in the ECHAM6 data set than in HAMMONIA, as it was mentioned in Sect. 3.1.
510 This and Fig.11 supports the idea that all self-excited oscillations have about the same vertical
511 amplitude structure.

512 The phase jumps in the nine oscillation vertical profiles of HAMMONIA also occur at
513 similar altitudes. Therefore the mean altitudes of these jumps have been calculated and are



514 shown in Fig.11 as blue horizontal arrows. They are seen to be close to the minima of the
515 accumulated amplitudes and thus confirm the anticorrelations between adjacent layers.
516 Figures 4, 1, and 11 thus show a general structure of temperature correlations/anticorrelations
517 between different layers of the HAMMONIA atmosphere, and suggest the phase structure of
518 the self-sustained oscillations as an explanation. The same is valid for ECHAM6.

519 Altogether HAMMONIA and ECHAM6 consistently show the same type of variability and
520 oscillation structures. This type occurs in a wide time domain of 400 years. As mentioned, we
521 do not believe that these ordered structures are adequately described by the term “noise”, as
522 this notion is normally used for something occurring at random.

523

524

525 3.3 Intrinsic oscillation periods

526

527 Three different model runs of different lengths have been investigated by the harmonic
528 analysis described. The HAMMONIA model covered 34 years, the WACCM model covered
529 150 years, and the ECHAM6 model covered 400 years. The intention was to study the
530 differences resulting from the different nature of the models, and from the difference in the
531 length of the model runs.

532 The oscillation periods found in these model runs are listed in Table 2. These periods are
533 vertical mean values as described for Fig.1 and Figs. 9-10. Periods are given in order of
534 increasing values in years together with their standard deviations. Only periods longer than 5
535 years are shown here. The maximum period cannot be longer than the length of the computer
536 run. Therefore, the number of periods to be found in a model run can -in principle- be the
537 larger the longer the length of the run is. Table 2 shows preferentially periods longer than 20
538 yr (except for HAMMONIA and Hohenpeißenberg) as the emphasis is on the long periods
539 here.

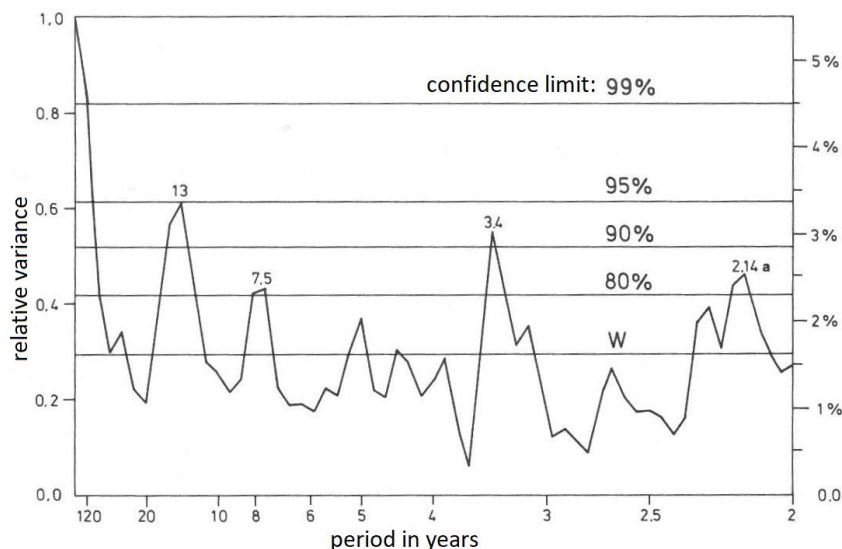
540 Table 2 also contains two rows of periods and their standard deviations that were derived
541 from *measured* temperatures. These are data obtained on the ground at the Hohenpeißenberg
542 Observatory (47.8°N, 11.0°E) from 1783 to 1980, and globally averaged GLOTI data (Global
543 Land Ocean Temperature Index, Hansen et al., 2010), respectively. The data are annual mean
544 values smoothed by a 16 point running mean and will be discussed below. Data after 1980 are
545 not included in the harmonic analyses because they steeply increase thereafter (“climate
546 change”). The periods are determined as for the zero level data of the other rows of Table 2
547 (see Section 3.2).

548 There are some empty spaces in the lists of Table 2. It is believed that this is because these
549 oscillations are not excited in that model run, or that their excitation is not strong enough to be
550 detected, or that the spectral resolution of the data series is insufficient (strong changes in
551 amplitudes strengths are, for instance, seen in Fig. 1.). For the *measured* data in Table 2 it
552 needs to be kept in mind that they were under the influence of varying boundary conditions.

553 The model runs shown in Table 2 have different altitude resolutions. The best resolution (1
554 km) is available in HAMMONIA (119 vertical layers, run Hhi-max in the earlier paper of
555 Offermann et al., 2015). The very long run of ECHAM6 uses only 47 layers. Data on a 3 km
556 altitude grid are used here. In the earlier paper it was shown on the basis of a limited data set
557 (HAMMONIA, Hlo-max) that a decrease of the number of layers affected the vertical
558 amplitude and phase profiles of the oscillations found. It did, however, not change the
559 oscillation periods. For a more detailed analysis a 20 year-long run of Hlo-max (67 layers) is
560 now compared to the 34 year-long run of Hhi-max (119 layers). The resulting oscillation
561 periods are shown in Table 3 (together with their standard deviations). Sixteen pairs of
562 periods are listed that all agree within the single error bars (except No. 4). Hence it is
563 confirmed that the periods of the oscillations are quite robust with respect to changes in



564 altitude resolution. The periods of the ECHAM6 run can therefore be considered as reliable,
565 despite their limited altitude resolution.
566
567



568
569 Fig.12 Periodogram (2 yr to 20 yr) of measured Hohenpeißenberg temperatures from
570 Schönwiese (1992, Abb.57). Results are from an autocorrelation spectral analysis ASA.
571

572 When comparing the periods in Table 2 to each other several surprising agreements are
573 observed. It turns out that all periods of the HAMMONIA and WACCM models find a
574 counterpart in the ECHAM6 data (not vice versa). These data pairs always agree within their
575 combined error bars, and mostly even within single error bars. The difference between the
576 members of a pair is much smaller than the distance to any neighbouring value with higher or
577 lower ordering number in Table 2. From this it is concluded that the different models find the
578 same oscillations. The periods of them are obviously quite robust. This and the fact that the
579 boundary conditions have been kept constant makes us believe that these oscillations are self-
580 sustained (intrinsic) oscillations.

581 A similar agreement is seen for the periods found in the measured Hohenpeißenberg data,
582 although these have been under the influence of variations of the sun, ocean, and greenhouse
583 gases. A spectral analysis (auto correlation spectral analysis ASA) of these data is shown in
584 Fig.12. It was taken from Schönwiese (1992). The important peak at 3.4 years is not
585 contained in Table 2, but was found in Offermann et al. (2015). The two peaks near 7.5 yr and
586 13 yr are close to the values 7.83 ± 0.26 yr and 13.6 ± 0.8 yr in Table 2.

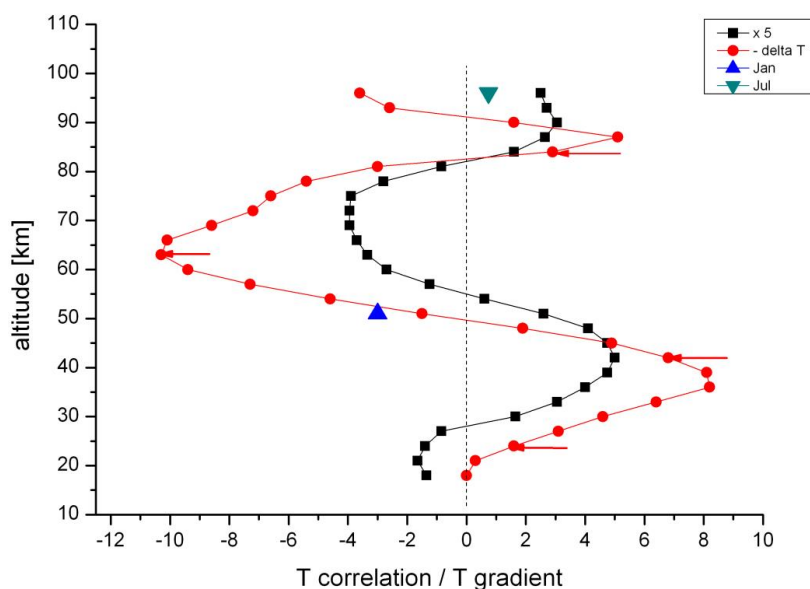
587 A 335 year long data set of Central England Temperatures (CET) is the longest measured
588 temperature series available (Plaut et al., 1995). A singular spectrum analysis was applied by
589 these authors for interannual and interdecadal periods. Periods of 25.0 yr, 14.2 yr, 7.7 yr, and
590 5.2 yr were identified. All of these values nearly agree with numbers given for HAMMONIA,
591 WACCM, and/or ECHAM6 in Table 2 (within the error bars given in the Table).

592 Meyer and Kantz (2019) recently studied the data from a large number of European stations
593 by the method of detrended fluctuation analysis. They identified a period of 7.6 ± 1.8 yr, which
594 again is in agreement with the HAMMONIA results given in Table 2 (and also agrees with
595 Fig.12, and with Plaut et al.,1995).

596
597



598 Also the GLOTI data in Table 2 are in agreement with some of the other periods, even
599 though they are global averages. The results altogether suggest that the periods discussed are
600 basic (intrinsic) properties of the atmosphere. It will be shown below that they are not limited
601 to atmospheric temperatures alone, but are, for instance, also seen in Methane mixing ratios.
602
603



604 Fig.13 Comparison of HAMMONIA vertical correlations from Fig.3 (black squares) with
605 vertical temperature gradients (red dots). Data are from annual mean temperatures.
606 Correlation coefficients are multiplied by 5. Temperature gradients are approximated by the
607 differences of consecutive temperatures (K per 3 km). Two gradients are given for monthly
608 mean temperature curves in addition: blue triangle for January, green inverted triangle for
609 July. Red arrows show the altitudes of the maxima of the accumulated amplitudes in Fig.11.
610
611

612 3.4 Oscillation amplitudes

613
614 In an attempt to learn more about the nature of the self-sustained oscillations we analyze
615 their oscillation amplitudes. The determination of absolute amplitudes of self-excited
616 oscillations is difficult and beyond the scope of the present paper. Nevertheless, interesting
617 results can be obtained from their relative values. One of these results is related to the vertical
618 gradients of the atmospheric temperature profiles.
619

620 The HAMMONIA model simulates the atmospheric structure as a whole. The annual mean
621 vertical profile of HAMMONIA temperatures can be derived and is seen to vary between a
622 minimum at the tropopause, a maximum at the stratopause, and another minimum near the
623 mesopause (not shown here). In consequence the vertical temperature gradients change from
624 positive to negative, and to positive again. This is shown in Fig.13 (red dots) between 18 km
625 and 96 km. The temperature gradients are approximated by the temperature differences of
626 consecutive levels.



627 Also shown in Fig.13 is the correlation profile of HAMMONIA from Fig.3 (black squares
628 here). The two curves are surprisingly similar (correlation coefficient is 0.80. Outside the
629 range shown the correspondence is lost.). The similarity suggests some connection of the
630 oscillation structure and the mean thermal structure of the middle atmosphere. This is
631 supported by the accumulated amplitudes of the self-excited oscillations in Fig.11. The
632 maxima of these occur at altitudes near to the extrema of the temperature gradients as is
633 shown by the red arrows in Fig. 13. The mechanism connecting the oscillations and the
634 thermal structure appears to be active throughout the whole altitude range shown (except the
635 lowest altitudes).

636 A possible mechanism might be a vertical displacement of air parcels. If an air parcel is
637 displaced vertically by some distance D (“displacement height”) a relative change in mixing
638 ratio is observed that can be estimated by the product $\{D \text{ times mixing ratio gradient}\}$. If the
639 vertical movement is an oscillation the trace gas variation is an oscillation as well, assuming
640 that D is a constant. Such transports may be best studied by means of a trace gas like CH_4 .

641 HAMMONIA methane mixing ratios have therefore been investigated for oscillation periods
642 in the same way as described above for the temperatures. Results are briefly summarized here.

643 Ten periods have been found, indeed, between 3.56 and 16.75 years by harmonic analyses.
644 These periods are very similar to those obtained for the temperatures in Table 2. The
645 agreement is within the single error bars. Hence it is concluded that the same self-sustained
646 oscillations are seen in HAMMONIA temperatures and CH_4 mixing ratios.

647 The CH_4 oscillations support the idea that a displacement mechanism is active. The
648 corresponding displacement heights D were estimated from the CH_4 amplitudes and the
649 vertical gradients of the mean HAMMONIA CH_4 mixing ratios.

650 The values D obtained from the different oscillation periods are about the same, though they
651 show some scatter. This means that the displacement mechanism is the same for all
652 oscillations. However, D appears to follow a trend in the vertical direction. The displacements
653 are below 100 m in the lower stratosphere and slowly increase with height to above 200 m.

654 Thus the important result is obtained that the self-sustained oscillations are related to a
655 vertical displacement mechanism that is altitude dependent, but appears to be the same for all
656 periods. A more detailed analysis is beyond the scope of this paper.

657

658

659 3.5 Seasonal aspects

660

661 Our analysis has so far been restricted to annual mean values. Large temperature variations
662 on much shorter time scales are also known to occur in the atmosphere, including vertical
663 correlations (e.g. seasonal variations). This suggests the question whether these might be
664 somehow related to the self-excited, long period oscillations. Our spectral analysis is therefore
665 repeated using monthly mean temperatures of HAMMONIA.

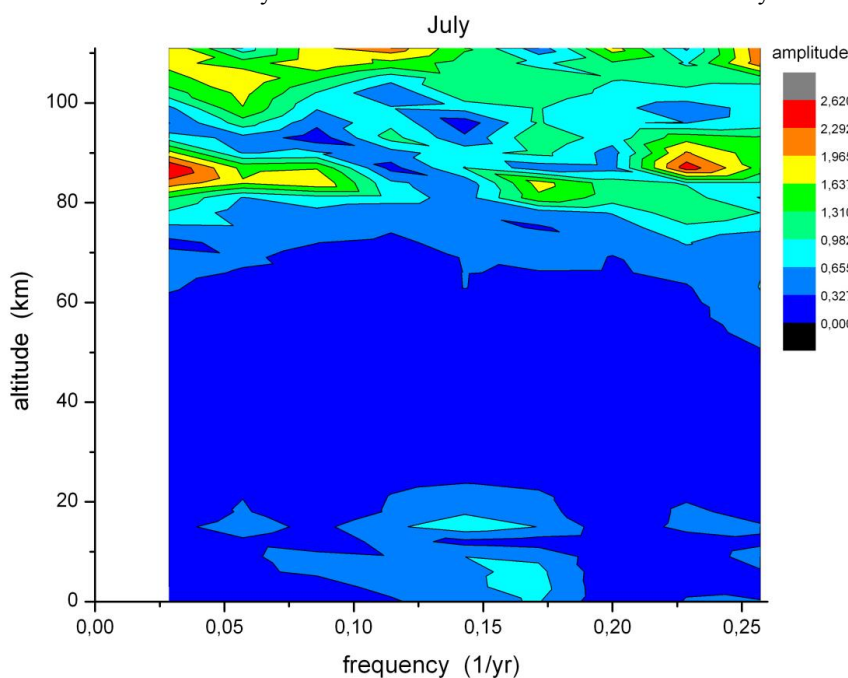
666 Results are shown in Fig. 14 and 15, which give the amplitude distribution vs period and
667 altitude of FFT analyses for the months of July and January. These two months are typical of
668 summer (May-August), and winter (November-March), respectively. In July oscillation
669 amplitudes are seen essentially at altitudes above about 80 km, and some below about 20 km.
670 In the regime in between, oscillations are obviously very small or not excited. The opposite
671 behaviour is seen in January: oscillation amplitudes are now observed in the middle altitude
672 regime where they had been absent in July. This is to be compared to Fig.6 and 11 that give
673 the annual mean picture. In Fig. 11 the structures (two peaks) above 80 km appear to
674 represent the summer months (Fig. 14). The structures between 80 km and 30 km, on the
675 other hand, apparently are representative of the winter months (Fig. 15).

676 The monthly oscillations appear to be linked to the wind field of the HAMMONIA model.
677 Figure 16 shows the monthly zonal winds of HAMMONIA from the ground up to 111 km



678 (50°N). Comparison with Fig. 14 and 15 shows that oscillation amplitudes are obviously not
679 observed in an easterly wind regime. Hence, the long period self-sustained oscillations and
680 their phase changes are apparently linked to the dynamical structure of the middle
681 atmosphere. A change from high to low oscillation activity in the vertical direction appears to
682 be linked to a wind reversal.

683 This correspondence does not, however, exist in all details. In the regimes of oscillation
684 activity there are substructures. For instance in the middle of the July regime of amplitudes
685 above 80 km there is a “valley” of low values at about 95 km. A similar valley is seen in the



686
687 Fig. 14 Self-excited temperature oscillations in the month of July in HAMMONIA.
688 Amplitudes are shown in dependence of altitude and frequency (periods 3.9-34 yr). Colour
689 code of amplitudes is in arbitrary units.

690
691
692 January data around 55 km. Near these altitudes there are phase changes of about 180° (see
693 the blue arrows in Fig.11). Contrary to our expectation sketched above, these are altitudes of
694 large westerly zonal wind speeds without much vertical change (see Fig.16). However, the
695 two “valleys” are relatively close to altitudes where the vertical temperature gradients are
696 small (see Fig.13). As the gradients from the annual mean temperatures used for the curves in
697 Fig.13 may differ somewhat from the corresponding monthly values two monthly gradients
698 have been added in Fig.13 for January (at 51 km) and at 96 km (for July). They are small,
699 indeed, and could explain low oscillation amplitudes by the above discussed vertical
700 displacement mechanism.

701

702

703 3.6 Oscillation persistence

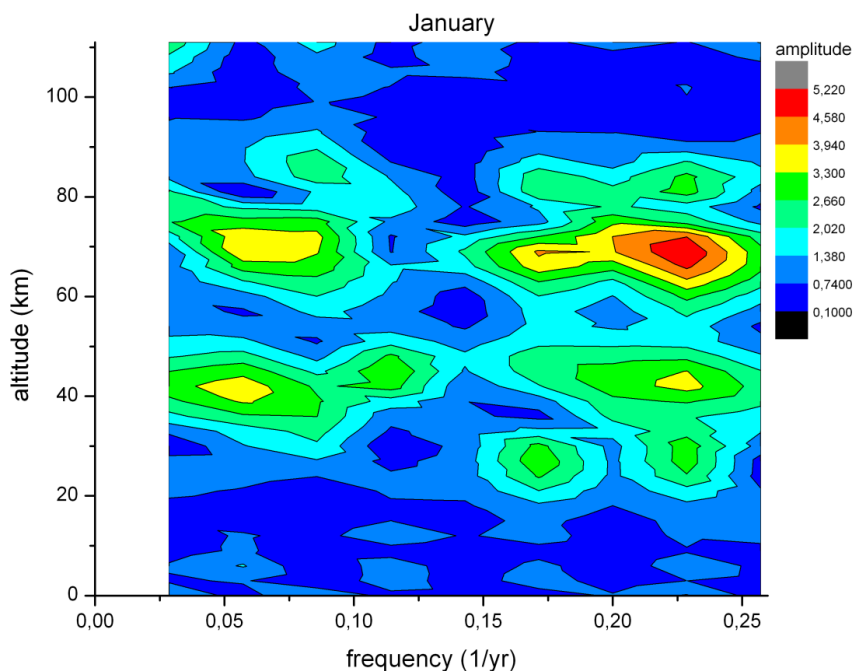
704

705 If our concept of self- excitation of oscillations is correct we might expect that such
706 oscillations might also dissipate after a while, i.e. we should expect some intermittance in our



707 oscillation amplitudes. To check on this we have subdivided the 400 years data record of
708 ECHAM6 in four smaller time intervals (blocks) of 100 years each. In each block we
709 performed harmonic analyses for periods of 24 yr (frequency 0.042/yr) and 37 yr (frequency
710 0.027/yr), respectively, at the altitudes of 42 km (1.9 hPa) and 63 km (0.11 hPa), respectively.
711 These are altitudes and periods with strong signals as seen in Fig.7. Results for the two
712 altitudes and two periods are given in Fig.17.

713 The results show two groups of amplitudes: one is around 0.15 K, the other is very small
714 and compatible with zero. The two groups are significantly different as is seen from the error
715 bars. This result is compatible with the picture of oscillations being excited and not-excited
716 (dissipated) at different times. The non-excitation (dissipation) for the 24 yr oscillation (black
717 squares) occurs in the first block (century), that for the 37 yr oscillation (red dots) in the
718 second block. The 24 yr profile at 63 km altitude is similar as that at 24 km. Likewise, the 37
719 yr profile at 24 km is similar to that at 63 km. Hence it appears that the whole atmosphere (or
720 a large part of it) is excited (or dissipated) simultaneously. (The two profiles in Fig.17 appear
721 to be somehow anticorrelated for some reason that is unknown as yet.)

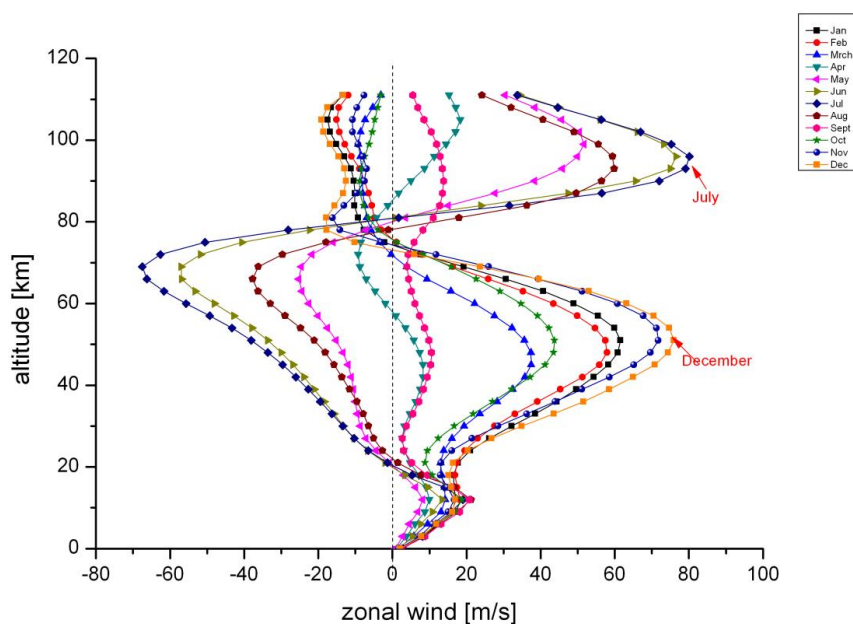


722
723 Fig. 15 Self-excited temperature oscillations as in Fig. 14, but for the month of January

724
725
726 For the analysis of shorter periods the 400 year data set of ECHAM6 may be subdivided in
727 a larger number of time intervals. Figure 18 shows the results for periods of 5.4 yr and 16 yr,
728 respectively, for various altitudes. An FFT analysis was performed in 12 equal time intervals
729 (blocks of 32 yr length) in the altitude regime 0.01 – 1000 hPa and the period regime 2 – 40
730 yr. The corresponding 12 maps look similar as Fig.15, i.e. there are pronounced amplitude hot
731 spots at various altitudes and periods. In subsequent blocks these hot spots may shift
732 somewhat in altitude and/or period, and hence the profiles taken at a fixed period and altitude
733 as those of Fig.18 show some scatter. Nevertheless, there is strong indication of the
734 occurrence of coordinated high maxima and deep minima of amplitudes in Blocks 3/ 4 and



735 Blocks 10/11, respectively. These maxima are interpreted as strong oscillation excitation,
736 whereas the minima are believed to show (at least in part) the dissipation of the oscillations.
737 It should be mentioned that in the FFT analysis the 5.4 yr period is an overtone of the 16 yr
738 period. Hence the two period data in Fig.18 may be somehow related.
739
740
741
742



743
744 Fig.16 Vertical distribution of zonal wind speed in the HAMMONIA model.
745

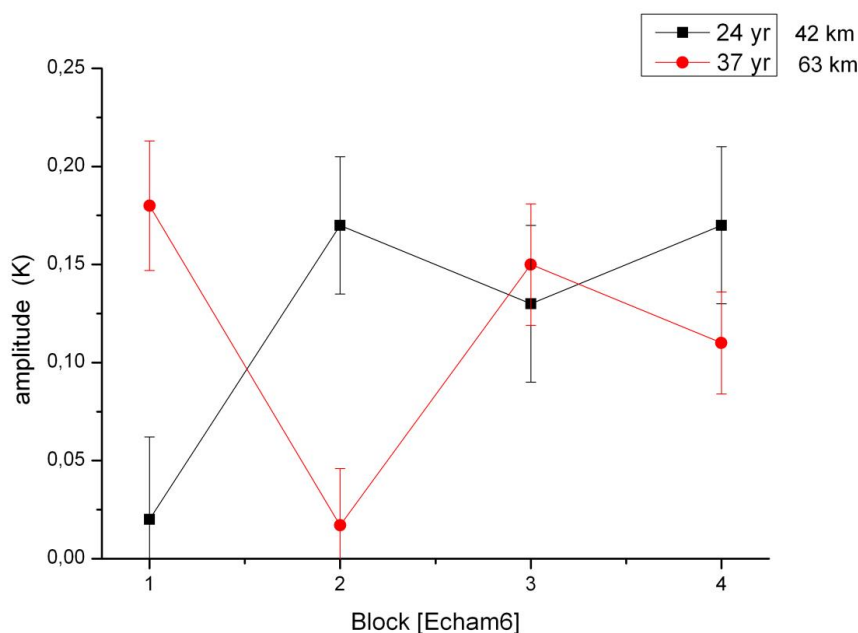
746 747 748 4 Discussion 749

750 4.1 The nature and origin of the self-sustained oscillations are as yet unknown. We
751 therefore collect here as many of their properties as possible. They do exist in computer
752 models even if the model boundaries for the influences of the sun, the ocean, and the green
753 house gases are kept constant. Therefore they are believed to be self-generated oscillations.
754 Further properties are as follows: The periods are robust, i.e. they are found with similar
755 values in different models. The periods cover a wide range from 2 to 341 years (at least). The
756 different oscillations have similar vertical profiles (up to 110 km) of amplitudes and phases.
757 This may indicate three-dimensional atmospheric oscillation modes. To clarify this, latitudinal
758 and longitudinal studies of the oscillations are needed in a future analysis.
759

760 4.2 The accumulated oscillation amplitudes show a layer structure with alternating maxima
761 and minima and correlations / anticorrelations in the vertical direction. These appear to be
762 influenced by the seasonal variations of temperature and zonal wind in the stratosphere,
763 mesosphere, and lower thermosphere. Table 4 summarizes the results shown in Section 3.5.



764 Maxima of oscillation amplitudes appear to be associated with westerly (eastward) winds
765 together with large temperature gradients (positive or negative). Amplitude minima are
766 associated with either easterly (westward) winds or with near zero temperature gradients. The
767 latter feature is compatible with a possible vertical displacement mechanism. Such
768 displacements can be seen, indeed, in the CH₄ data of the HAMMONIA model. The
769 mechanism summarized in Table 4 appears to be a
770



771
772

773 Fig.17 Amplitudes of 24 yr and 37 yr oscillations in four subsequent equal time intervals
774 (Blocks) of the 400 year data set of ECHAM6.

775
776

777 basic feature of the atmosphere that influences many different parameters as temperature,
778 mixing ratios, etc.. Vertical displacements of measured temperature profiles have been
779 discussed for instance by Kalicinsky et al.(2018).

780

781 4.3 The amplitudes found for the self-sustained oscillations are relatively small (Fig.1). The
782 question therefore arises whether these oscillations might be spurious peaks, i.e. some sort of
783 noise. We tend to deny the question for the following reasons:

784

785 (a) An accidental agreement of periods as close together as those shown in Table 2 for
786 different model computations appears very unlikely. This also applies to the Hohenpeißenberg
787 data in Table 2, and several of these periods are even found in the GLOTI data.

788

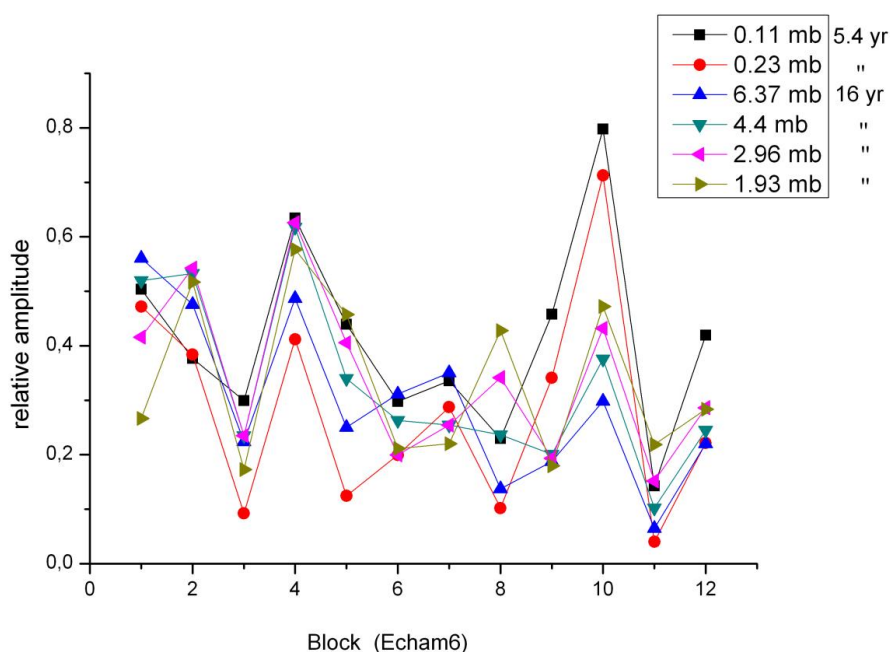
789 If the period values were accidental they should be evenly distributed over the
790 period- space. To study this the range of ECHAM6 periods (20 – 341 yr) is
791 considered. Table 2 shows that the error bars (standard deviations) of ECHAM6
792 cover approximately half of this range. If the periods of this and some other data set occur at
random, half of them should coincide with the ECHAM6 periods within the



793 ECHAM6 error bars, and half of them should not. This is checked by means of the
794 WACCM model data, the Hohenpeissenberg measured data, and three further
795 measurements sets that reach back to 1783 (Innsbruck, 47.3°N;11.4°E; Vienna,
796 48.3°N;16.4°E; Stockholm, 59.4°N;18.1°E). The result is that about two thirds of the
797 periods coincide with ECHAM6 periods within the ECHAM6 error bars. This is far
798 from an even distribution.

799 It is important to note that the data sets used here are quite different in nature: They are
800 either model simulations with fixed or partially fixed boundaries, or they are real atmospheric
801 measurements at different locations.

802
803



804
805
806
807
808
809

Fig.18 FFT amplitudes of 5.4 yr and 16 yr oscillations in 12 equal time intervals (32 yr blocks) of the ECHAM6 400 year data set.

810 A further argument against noise is the distribution of the data in Fig. 9 and 10. If our
811 oscillations were noise, the peaks in these Figures should be evenly distributed with respect to
812 the period scale. However, the distribution is highly uneven, with high peaks and large gaps,
813 which is very unlikely to result from noise.

814

815 (b) The periods given in Table 2 were all calculated by means of harmonic analyses. This
816 was done to support the reliability of the comparison of the three models and four
817 measured data sets. There could be, however, the risk of a “common mode failure”. The
818 harmonic analysis results are therefore checked, and are confirmed by the Lomb-
819 Scargle and autocorrelative spectral (ASA) analyses shown in Fig.8 and 12, and by the above
820 cited results of Plaut et al.,(1995) and Meyer and Kantz (2019). There is, however, not a one-
821 to-one correspondence of these numbers and those of Table2. In general the number of



822 oscillations found by the harmonic analysis is larger. Hence several of the Table 2 periods
823 might be considered questionable. It is also not certain that Table 2 is exhaustive.
824 Nevertheless, the large number of close coincidences is surprising.

825
826 (c) The layered structure of the occurrence of the oscillations (e.g. Fig.11) and the
827 corresponding anti-correlations appear impossible to reconcile with a noise field. These
828 correlations extend over about 20 km (or more) in the vertical which is about three scale
829 heights. Turbulent correlation would, however, be expected over one transport length, i.e. one
830 scale height, only.

831
832 (d) The apparent link of the oscillations to the zonal wind field and the vertical
833 temperature structure (Table 4) would be very difficult to be explained by noise.

834
835 (e) The close agreement (within single error bars) of the oscillation periods in
836 temperatures and in CH₄ mixing ratios would also be very difficult to be explained by
837 noise.

838
839 In summary it appears that many of the oscillations are intrinsic properties of the
840 atmosphere that are also found in sophisticated simulations of the atmosphere.

841

842

843 4.4 The self-sustained oscillations are studied here mainly for atmospheric temperatures.
844 They show up, however, in a similar way in other parameters as winds, pressure, trace gas
845 densities, NAO, etc. (Offermann et al., 2015). Some of the periods in Table 2 appear to be
846 similar to the internal decadal variability of the atmosphere/ocean system (e.g., Meehl et al.,
847 2013; 2016; Fyfe et al. 2016). One example is the Atlantic Multidecadal Oscillation (AMO)
848 as discussed by Deser et al.(2010) with time scales of 65-80 yr, and with its “precise nature
849 ...still being refined”. Variability on centennial time scales and its internal forcing was
850 recently discussed by Dijkstra and von der Heydt (2017). It needs to be emphasized that the
851 oscillations discussed in the present paper are not influenced by the ocean as they occur even
852 if the ocean boundaries are kept constant.

853

854 4.5 The self-sustained oscillations obviously are somehow related to the “internal
855 variability” discussed in the atmosphere/ocean literature at 40 – 80 years time scales (“climate
856 noise”, see e.g. Deser et al., 2012, Gray et al., 2004, and other references in Section 1). The
857 particular result of the present analysis is its extent from the ground up to 110 km, showing
858 systematic structures in all of this altitude regime. These vertical structures lead us to hope
859 that the nature of the oscillations and hence of (part of) the “internal variability” can be
860 revealed in the future.

861

862 4.6 It appears that the time persistency of the self-sustained oscillations is limited. Longer
863 data sets are needed to study this further.

864

865 4.7 The internal variability in the atmosphere/ocean system “...makes an appreciable
866 contribution to the total... uncertainty in the future (simulated) climate response...” (Deser et
867 al., 2012). Similarly our self-sustained oscillations might interfere with long term (trend)
868 analyses of various atmospheric parameters. This includes slow temperature increases as part
869 of the long term climate change, and needs to be studied further.

870

871

872



873
874
875
876
877
878
879
880
881
882
883
884
885
886
887
888
889
890
891
892
893
894
895
896
897
898
899
900
901
902
903
904
905
906
907
908
909
910
911
912
913
914
915
916
917
918
919
920
921
922
923

5 Summary and Conclusions

The structures analyzed in this paper are believed to be oscillations that are self-generated (self-sustained) in the atmosphere. The oscillations occur in a similar way in different atmospheric climate models, and even if the boundary conditions of sun, ocean, and greenhouse gases are kept constant. They also occur in long-term temperature measurements series. They are characterized by a large range of period values from below 5 to beyond 300 years. Periods of self-excited oscillations are known to be robust. This is in line with the fact that we find very nearly the same periods in different climate model calculations as well as in long observation series.

As we do not yet understand the nature of the oscillation structures we try to assemble as many of their properties as possible. The oscillations show typical and consistent structures in their vertical profiles. Temperature amplitudes show a layered behaviour in the vertical direction with alternating maxima and minima. Phase profiles are also layered with 180° phase jumps near the altitudes of the amplitude minima (anticorrelations). There are also indications of vertical transports suggesting a displacement mechanism in the atmosphere. As an important result we find that for all oscillation periods the altitude profiles of amplitudes and phases as well as the displacement heights are nearly the same. This leads us to suspect an atmospheric oscillation mode.

These signatures are found to be linked to the thermal and dynamical structure of the middle atmosphere. They are seen to be an essential part of atmospheric dynamics. All results presently available are local, i.e. they refer to the latitude and longitude of Central Europe. In a future step horizontal investigations need to be performed to check on a possible modal structure.

Most of the present results are for temperatures at various altitudes (up to 110 km). Other atmospheric parameters indicate a similar behaviour and need to be analyzed in detail in the future. Also, the potential of the long period oscillations to interfere with trend analyses needs to be investigated.



924
925
926 Author contribution
927
928
929 DO performed data analysis and prepared the manuscript and figures with contributions from
930 all co-authors.
931
932 JW managed data collection and performed FFT spectral analyses.
933
934 ChK performed Lomb-Scargle spectral and statistical analyses
935
936 RK provided interpretation and editing of the manuscript, figures, and references.
937
938
939
940
941 Competing Interests
942
943
944 The authors declare that they have no conflict of interest.
945
946
947
948
949
950
951
952
953
954
955
956
957
958
959
960
961
962
963
964
965
966
967
968
969
970
971
972
973
974



975
976
977 Acknowledgements
978
979
980
981 Global Land Ocean Temperature Index (GLOTI) data were downloaded from
982 http://data.giss.nasa.gov/gistemp/tabledata_v3/GLB.Ts+dSST.txt and are gratefully
983 acknowledged..
984
985 We thank Katja Matthes (GEOMAR, Kiel, Germany) for making available the WACCM4
986 data, and for helpful discussions. Model integrations of the CESM-WACCM Model have
987 been performed at the Deutsches Klimarechenzentrum (DKRZ) Hamburg, Germany. The help
988 of Sebastian Wahl in preparing the CESM-WACCM data is greatly appreciated.
989
990 HAMMONIA and ECHAM6 simulations were performed at and supported by the German
991 Climate Computing Centre (DKRZ). Many and helpful discussions with Hauke Schmidt (MPI
992 Meteorology, Hamburg, Germany) are gratefully acknowledged.
993
994 We are grateful to Wolfgang Steinbrecht (DWD, Hohenpeißenberg Observatory, Germany)
995 for the Hohenpeißenberg data and many helpful discussions.
996
997 Part of this work was funded within the project MALODY of the ROMIC program of the
998
999 German Ministry of Education and Research under Grant No. 01LG1207A
1000
1001
1002
1003
1004
1005
1006
1007
1008
1009
1010



- 1011
1012
1013 References.
1014
1015 Biondi, F., Gershunov, A., and Cayan, D.R.: North Pacific Decadal Climate Variability since
1016 1661, *J. Climate* 14, 5-10, 2001.
1017
1018 Dai, A, Fyfe, J.C., Xie, Sh.-P., and Dai, X.: 2015.: Decadal modulation of global surface
1019 temperature by internal climate variability, *Nature Climate Change*,
1020 doi:10.1036/NCLIMATE2605 , 2015.
1021
1022 Deser, C. Alexander, M.A., Xie,S.P., Phillips, A.S.: Sea surface temperature variability:
1023 patterns and mechanisms, *Ann. Rev. Mar. Sci.*,2, 115-143, 2010.
1024
1025 Deser, C., Phillips, A., Bourdette, V., and Teng, H.: Uncertainty in climate change
1026 projections: the role of internal variability, *Clim. Dyn.*, 38, 527-546, 2012.
1027
1028 Deser, C., Phillips, A.S., Alexander, M.A., and Smoliak, B.V.: Projecting North American
1029 climate over the next 50 years: Uncertainty due to internal variability, *J.Climate*, 27, 2271-
1030 2296, 2014.
1031
1032 Dijkstra, H.A., te Raa, L., Schmeits, M., and Gerrits, J.: On the physics of the Atlantic
1033 Multidecadal Oscillation, *Ocean Dynamics*, DOI: 10/1007/s10236-005-0043-0, 2005.
1034
1035 Dijkstra, H.A., and von der Heydt, A.S.: Basic mechanisms of centennial climate variability,
1036 *Pages Magazine*, Vol.25, No.3, 2017.
1037
1038 Flato, G., et al. : Evaluation of Climate Models, in: *Climate Change 2013: The Physical*
1039 *Science Basis, Contribution of Working Group I to the Fifth Assessment Report of the*
1040 *Intergovernmental Panel on Climate Change*, (eds..Stocker, T.E., et al.) Ch.9, IPCC,
1041 Cambridge Univ.Press, UK and New York, NY, USA, 2013.
1042
1043 Fyfe, J. C., Meehl, G.A., England, M.H., Mann, M.E., Santer, B.D., Flato, G.M., Hawkins,
1044 E., Gillett, N.P., Xie, Sh.P., Kosaka, Y., and Swart, N.C.: Making sense of the early-2000s
1045 warming slowdown, *Nature Climate Change*, 6, 224-228, 2016.
1046
1047 Giorgetta, M. et al.: Climate and carbon cycle changes from 1850 to 2100 in MPI-ESM
1048 simulations for the coupled model intercomparison project phase 5, *J. Adv. Model. Earth*
1049 *Syst*, 5, 572-597, doi:10.1002/jame.20038, 2013.
1050
1051 Gray, ST.T., Graumlich, L.J., Betancourt, J.L., and Pederson, G.T.: A tree-ring based
1052 reconstruction of the Atlantic Multidecadal Oscillation since 1567 A.D.. *Geophys.Res.Lett.*,
1053 31, L 12205, doi:10.1029/2004GL019932 2004.
1054
1055 Hansen, F., Matthes, K., Petrick, C., and Wang, W.: 2014. The influence of natural and
1056 anthropogenic factors on major stratospheric sudden warmings. *J.Geophys.Res. Atmos.*, 119,
1057 8117-8136, 2014.
1058
1059 Hansen, J., Ruedy, Sato, M., and Lo, K.: Global Surface Temperature Change, *Rev.Geophys.*,
1060 48, RG 4004, 2010.
1061 .



- 1062 Kalicinsky, Ch., Knieling, P., Koppmann, R., Offermann, D., Steinbrecht, W., and Wintel,
1063 J.: 2016. Long term dynamics of OH* temperatures over Middle Europe: Trends and solar
1064 correlations, *Atmos. Chem. Phys.*, 16, 15033 – 15047, 2016.
1065
- 1066 Kalicinsky, CH., Peters, D.H.W., Entzian, G., Knieling, P., and Matthias, V.: Observational
1067 evidence for a quasi-bidecadal oscillation in the summer mesopause region over Western
1068 Europe, *J. Atmos. Sol.-Terr. Phys.*, 178, 7 – 16., doi.org/10.1016/j.jastp.2018.05.008, 2018.
1069
- 1070 Karnauskas, K. B., Smerdon, J.E., Seager, R., and Gonzalez-Rouco, J.F. : A pacific centennial
1071 oscillation predicted by coupled GCMs, *JCLI* September 2012, doi:10.1175/JCLI-D-11-
1072 00421.1, 2012.
1073
- 1074 Kinnison, D., Brasseur, G.P., Walters, S., et al.: Sensitivity of chemical tracers to
1075 meteorological parameters in the MOZART-3 chemical transport model. *J.Geophys.Res.*,
1076 112, D20302, doi :10.1029/2006JD007879, 2007.
1077
- 1078 Latif, M., Martin, T., and Park, W.: Southern ocean sector centennial climate variability and
1079 recent decadal trends, *J. Climate*, 26, 7767-7782, 2013.
1080
- 1081 Lean,J., Rottman, G., Harder, J., and G.Knopp, G.: SOURCE contributions to new
1082 understanding of global change and solar variability, *Sol.Phys.* 230, 27-53.
1083 doi:10.1007/S11207-005-1527-2, 2005.
1084
- 1085 Lomb, N.R., Least-squares frequency analysis of unequally spaced data, *Astrophys.Space*
1086 *Sci.*, 39, 447-462, 1976.
1087
- 1088 Lu, J., Hu, A., and Zeng, Z.: On the possible interaction between internal climate variability
1089 and forced climate change, *Geophys. Res. Lett.*, 41, 2962-2970, 2014.
1090
- 1091 Mantua, N.J., and Hare, St.R.: The Pacific Decadal Oscillation. *J.Oceanography*, 58, 35,2002.
1092
- 1093 Matthes, K., Kodera, K., Garcia, R.R., Kuroda, Y., Marsh, D.R., and Labitzke, K.: The
1094 importance of time-varying forcing for QBO modulation of the atmospheric 11 year solar
1095 cycle signal, *J.Geophys.Res.*, 118, 4435-4447, 2013.
1096
- 1097 Meehl, G.A., Hu, A., Arblaster, J., Fasullo, J., and Trenberth, K.E.: Externally forced and
1098 internally generated decadal climate variability associated with the Interdecadal Pacific
1099 Oscillation, *J.Climate*, 26, 7298-7310, 2013.
1100
- 1101 Meehl, G.A., Hu, A., Santer, B.D., and Xie, SH.-P.: Contribution of Interdecadal Pacific
1102 Oscillation to twentieth-century global surface temperature trends. *Nature Climate Change*,
1103 6,1005-1008, doi:10.1038/nclimate3107, 2016.
1104
- 1105 Meyer, P.G., and Kantz, H.: A simple decomposition of European temperature variability
1106 capturing the variance from days to a decade, *Climate Dynamics*, 53, 6909-6917,
1107 doi.org/10.1007/s00382-019-04965-0, 2019.
1108
- 1109 Minobe, Sh.: A 50-70 year climatic oscillation over the North Pacific and North America,
1110 *Geophys.Res.Lett.*, 24, 683-686, 1997.
1111



- 1112 Offermann, D., Goussev, O., Kalicinsky, Ch., Koppmann, R., Matthes, K., Schmidt, H.,
1113 Steinbrecht, W., and J. Wintel, J.: A case study of multi-annual temperature oscillations in
1114 the atmosphere: Middle Europe, *J.Atmos.Sol.-Terr.Phys.*, 135, 1-11, 2015.
1115
- 1116 Plaut, G., Ghil, M., and Vautard, R.: Interannual and interdecadal variability in 335 years of
1117 Central England Temperatures, *Science*, 268, 710 – 713, 1995.
1118
- 1119 Paul, A., and M. Schulz, M.: Holocene climate variability on centennial-to-millennial time
1120 scales: 2. Internal and forced oscillations as possible causes. In: Wefer,G., W.Berger, K-E.
1121 Behre, and E. Jansen (eds), 2002, *Climate development and history of the North Atlantic*
1122 *realm*, Springer, Berlin, Heidelberg, 55-73, 2002.
1123
- 1124 Pikovsky, A., Rosenblum, M., Kurths, J., *Synchronization - A universal concept in nonlinear*
1125 *science*, Cambridge University Press, Cambridge, UK, 2003.
1126
- 1127 Polyakov,I.V. Berkryaev, R.V., Alekseev,G.V., Bhatt, U.S., Colony, R.L., Johnson, M.A.,
1128 Maskshitas, A.P., and Walsh, D.: Variability and trends of air temperature and pressure in the
1129 *Maritime Arctic, 1875-2000*, *J.Climate*, 16, 2067-2077, 2003.
1130
- 1131 Roeckner, E., Brokopf, R., Esch, M., Giorgetta, M., Hagemann, S., Kornblueh, L., Manzini,
1132 E., Schlese, U., Schulzweida, U.: Sensitivity of simulated climate to horizontal and vertical
1133 resolution in the ECHAM5 atmosphere model, *J.Clim.*, 19, 3771–3791, 2006.
1134
- 1135 Scargle, J.D.: Studies in astronomical time series analysis. II. Statistical aspects of spectral
1136 analysis of unevenly spaced data, *Astrophys.J.*, 263, 835-853, 1982.
1137
- 1138 Schlesinger, M.E. and N. Ramankutty, N.: An oscillation in the global climate system of
1139 period 65-70 years, *Nature*, 367, 723-726, 1994.
1140
- 1141 Schmidt, H., Brasseur, G.P., Charron, M., Manzini, E., Giorgetta, M.A., Diehl,T., Fo-
1142 michev, V.I., Kinnison, D., Marsh, D., Walters, S.: The HAMMONIA chemistry climate
1143 model: Sensitivity of the mesopause region to the 11-year solar cycle and CO2 doubling, *J.*
1144 *Clim.*, 19, 3903–3931, <http://dx.doi.org/10.1175/JCLI3829.1>, 2006.
1145
- 1146 Schmidt, H., Brasseur, G.P., and Giorgetta, M.A.:2010. The solar cycle signal in a general
1147 circulation and chemistry model with internally generated quasi-biennial oscillation. *J.*
1148 *Geophys. Res.* 115, 8, doi :10.1029/2009JD012542, 2010.
1149
- 1150 Schönwiese, Ch.-D.: *Praktische Statistik für Meteorologen und Geowissenschaftler*,
1151 *2.Auflage*, Gebrüder Borntraeger, Berlin, Stuttgart, Abb.57, page 185, [www.borntraeger-](http://www.borntraeger-cramer.de/9783443010294)
1152 [cramer.de/9783443010294](http://www.borntraeger-cramer.de/9783443010294), 1992.
1153
- 1154 Soon, W. W.-H.: Variable solar irradiance as a plausible agent for multidecadal variations in
1155 the Arctic-wide surface air temperature record of the past 130 years, *Geophys.Res.Lett.*, 32,
1156 L16712, doi:10.1029/2005GL023429 2005.
1157
- 1158 Stevens, B., Giorgetta, M., Esch, M., Mauritsen, T., Crueger, T., Rast, S., Salzmann, M.,
1159 Schmidt, H., Bader, J., Block, K., Brokopf, R., Fast, I., Kinne, S., Kornblueh, L., Lohmann,
1160 U., Pincus, R., Reichler, T., and Roeckner, E.: The atmospheric component of the MPI-M
1161 earth system model: ECHAM6, *J. Adv. Model. Earth Syst.*, 5, 1-27, 2013.
1162



1163 White, W.B., and Liu, Z.: Non-linear alignment of El Nino to the 11-yr solar cycle,
1164 Geophys.Res.Lett., 35, L19607, doi:10.1029/2008GL034831, 2008.
1165
1166 Xu, D., Lu, H., Chu, G., Wu, N., Shen, C., Wang, C., and Mao, L.: 500-year climate cycles
1167 stacking of recent centennial warming documented in an East Asian pollen record,
1168 Scientific Reports , 4, No.3611, doi:10.1038/srep03611, 2014.
1169
1170
1171
1172
1173
1174
1175
1176
1177
1178
1179
1180
1181
1182
1183
1184
1185
1186
1187
1188
1189
1190
1191
1192
1193
1194
1195
1196
1197
1198
1199
1200
1201
1202
1203
1204
1205
1206
1207
1208
1209
1210
1211
1212
1213
1214



1215
 1216
 1217
 1218
 1219
 1220
 1221
 1222
 1223
 1224
 1225
 1226
 1227
 1228
 1229
 1230
 1231
 1232
 1233
 1234
 1235
 1236
 1237
 1238
 1239
 1240
 1241
 1242
 1243
 1244
 1245
 1246
 1247
 1248
 1249
 1250
 1251
 1252
 1253
 1254
 1255
 1256
 1257
 1258
 1259
 1260
 1261
 1262
 1263
 1264
 1265
 1266
 1267
 1268
 1269
 1270
 1271

Table 1

Properties of the GCM simulations

All data are for Central Europe (50°N, 7°E), for details see text.

	HAMMONIA	WACCM4	ECHAM6
Horizontal resolution	T31	1.9°x2.5° (lat/long)	T63
Vertical resolution	119 levels 1 km (stratosphere)	66 levels	47 levels
altitude range	0 – 110 km	0 – 108 km	0 – 78 km
length of simulation	34 yr	150 yr	400 yr
time resolution of data used	annual/monthly	annual	annual
boundary conditions			
- sun	fixed	variable (see text)	fixed
- ocean	SST fixed	climatological SST and sea ice	fixed
- greenhouse gases	fixed	fixed (1960 values)	fixed
References	Schmidt et al., 2010	Hansen et al., 2014	Stevens et al., 2013



1272
 1273
 1274
 1275
 1276
 1277
 1278
 1279
 1280
 1281
 1282
 1283
 1284
 1285
 1286
 1287
 1288
 1289
 1290
 1291
 1292
 1293
 1294
 1295
 1296
 1297
 1298
 1299
 1300
 1301
 1302
 1303
 1304
 1305
 1306
 1307
 1308
 1309
 1310
 1311
 1312
 1313
 1314
 1315
 1316
 1317
 1318
 1319
 1320
 1321
 1322
 1323
 1324

Table 2:

Periods of temperature oscillations from harmonic analyses

Periods are numbered according to increasing values. Periods (in years) are given with their standard deviations. Self-sustained periods are from the HAMMONIA, WACCM, and ECHAM6 models, respectively. Additional periods are from Hohenpeißenberg measurements, and from the Global Land Ocean Temperature Index (GLOTI).

HAMMONIA periods are limited to 28.5 yr as the model run covered 34 yr, only.

WACCM periods are given below 147 yr from a model run of 150 yr. ECHAM6 periods are from a 400 yr run.

Short periods (below 20 yr) are not shown for WACCM, ECHAM6, and GLOTI as they are not used in the present paper. Hohenpeißenberg and GLOTI data after 1980 are not included in the analyses because of their steep increase in later years.

Periods given in bold type are significant at the 1 – 2 σ level or better, or are confirmed in the literature.

No	HAMMONIA (119 layers) (years)		WACCM (years)		ECHAM6 (47 layers) (years)		Hohenpeißenberg 1783 – 1980 (years)		GLOTI 1880 - 1980 (years)	
1	5.34	± 0.1					5.48	±0.21		
2	6.56	0.24					6.16	0.20		
3	7.76	0.29					7.83	0.26		
4	9.21	0.53					9.50	0.65		
5	10.8	0.34					10.85	0.38		
6	13.4	0.68					13.6	0.80		
7	17.3	1.05					18.02	1.08		
8	--	--			20.0	±0.35	19.9	± 1	20.2 ± 1.36	
9	--	--			20.9	0.15	--	--		
10	22.8	1.27	21.7 ± 1.02		22.1	0.23	21.9	0.94		
11	--	--			23.8	0.42				
12	--	--	25.82	0.86	25.3	0.46	25.1	0.62	25.5 2.0	
13	28.5	1.63	--	--	27.3	0.41	--	--		
14			31.56	1.42	30.2	0.49	29.8	0.66		
15			--	--	33.3	0.84	--	--		
16			38.1	0.82	36.9	1.17	36.01	1.28	35.4 2.42	
17			41.89	0.95	41.4	0.97	--	--		
18			--	--	48.4	1.73	--	--		
19			--	--	--	--	52.06	1.61	53.4 11.4	
20			57.64	1.69	58.3	1.77	--	--		
21			66.95	7.31	64.9	2.98	--	--		
22			--	--	77.5	3.94	81.6	4.18		
23			97.27	5.06	95.5	5.86	--	--		
24			147	14.9	129.4	14.5	--	--		
25					206.7	16.3	--	--		
26					--	--	238.2	11.8		
27					341.2	37.2				



1325
1326
1327
1328
1329
1330
1331
1332
1333
1334
1335
1336
1337
1338
1339
1340
1341
1342
1343
1344
1345
1346
1347
1348
1349
1350
1351
1352
1353
1354
1355
1356
1357
1358
1359
1360
1361
1362
1363
1364
1365
1366
1367
1368
1369
1370
1371
1372
1373
1374
1375
1376

Table 3

Period comparison of two different HAMMONIA runs

Periods (in years) are given together with their standard deviations.

HAMMONIA run Hhi-max uses 119 altitude layers and covers 34 years; run Hlo-max uses 67 layers and covers 20 years.

No	Hhi-max	Hlo-max
1	2.06 ± 0.02	2.07 ± 0.04
2	2.16 0.02	2.15 0.02
3	2.33 0.04	2.36 0.03
4	2.51 0.04	2.43 0.02
5	2.79 0.08	2.78 0.07
6	3.11 0.08	3.2 0.09
7	3.52 0.12	3.44 0.15
8	3.96 0.08	3.9 0.12
9	4.48 0.21	4.27 0.21
10	5.34 0.1	5.48 0.29
11	6.56 0.24	6.57 0.29
12	7.76 0.29	8.02 0.12
13	9.21 0.53	9.16 0.33
14	10.8 0.34	11.05 0.46
15	13.4 0.68	13.02 0.83
16	17.3 1.05	-- --
17	22.8 1.27	22.68 1.11



1377

1378

1379 Table 4

1380

1381 Maxima / minima of accumulated amplitudes of temperature oscillations and
1382 associated structures (see Fig.11)

1383 (stratosphere, mesosphere, lower thermosphere)

1384

1385

1386

1387 altitude accumulated zonal wind temperature gradient

1388 (km) amplitudes

1389

1390 105 max westerly (summer) large (positive)

1391

1392 93 min westerly (summer) near zero

1393

1394 84 max westerly (summer) large (positive)

1395

1396 78 min easterly (except Sept) medium (negative)

1397

1398 63 max westerly (winter) large (negative)

1399

1400 51 min westerly (winter) near zero

1401

1402 42 max westerly (winter) large (positive)

1403

1404

1405

1406

1407

1408

1409

1410

1411

1412

1413

1414

1415

1416

1417

1418

1419

1420

1421

1422

1423

1424

1425

1426

1427



1428
1429
1430
1431
1432
1433
1434
1435
1436
1437
1438
1439
1440
1441
1442
1443
1444
1445
1446
1447
1448
1449
1450
1451
1452
1453
1454
1455
1456
1457
1458
1459
1460
1461
1462
1463
1464
1465
1466
1467
1468
1469
1470
1471
1472
1473
1474
1475
1476
1477
1478
1479
1480
1481
1482
1483
1484

Table 5

List of Acronyms

Acronym

Definition

CCM	Chemistry Climate Model
CESM-WACCM	Community Earth System Model – Whole Atmosphere Community Climate Model
ECHAM6	ECMWF/Hamburg
GLOTI	Global Land Ocean Temperature Index
HAMMONIA	HAMBURG Model of the Neutral and Ionized Atmosphere
IPCC	Intergovernmental Panel on Climate Change
LOTI	Land Ocean Temperature Index